Monthly Notices
of the
ROYAL ASTRONOMICAL SOCIETY

MNRAS **439,** 2638–2650 (2014)
Advance Access publication 2014 February 18

doi:10.1093/mnras/stu118

Chemical abundances in bright giants of the globular cluster M62 (NGC 6266)★

David Yong,[1]†‡ Alan Alves Brito,[1,2] Gary S. Da Costa,[1] Javier Alonso-García,[3,4] Amanda I. Karakas,[1] Marco Pignatari,[5] Ian U. Roederer,[6] Wako Aoki,[7] Cherie K. Fishlock,[1] Frank Grundahl[8] and John E. Norris[1]

[1]*Research School of Astronomy and Astrophysics, Australian National University, Canberra, ACT 2611, Australia*
[2]*Instituto de Física, Universidade Federal do Rio Grande do Sul, 91501-970 Porto Alegre, RS, Brazil*
[3]*Instituto de Astrofísica, Facultad de Física, Pontificia Universidad Católica de Chile, Av. Vicuña Mackenna 4860, 782-0436 Macul, Santiago, Chile*
[4]*The Milky Way Millennium Nucleus, Av. Vicuña Mackenna 4860, 782-0436 Macul, Santiago, Chile*
[5]*Department of Physics, University of Basel, Klingelbergstrasse 82, CH-4056 Basel, Switzerland*
[6]*Department of Astronomy, University of Michigan, 500 Church Street, Ann Arbor, MI 48109, USA*
[7]*National Astronomical Observatory, Mitaka, Tokyo 181-8588, Japan*
[8]*Stellar Astrophysics Centre, Department of Physics and Astronomy, Aarhus University, Ny Munkegade 120, DK-8000 Aarhus C, Denmark*

Accepted 2014 January 15. Received 2014 January 14; in original form 2013 November 26

ABSTRACT

With the exception of Terzan 5, all the Galactic globular clusters that possess significant metallicity spreads, such as ω Cen and M22, are preferentially the more luminous clusters with extended horizontal branches. Here we present radial velocities and chemical abundances for seven bright giants in the globular cluster M62, a previously little-studied cluster. With $M_V = -9.18$, M62 is the ninth most luminous Galactic globular cluster and has an extended horizontal branch. Within our sample, we find (i) no evidence for a dispersion in metallicity, [Fe/H], beyond the measurement uncertainties, (ii) star-to-star abundance variations for C, O, Na and Al with the usual correlations between these elements as seen in other globular clusters, and (iii) a global enrichment for the elements Zr, Ba and La at the level [X/Fe] $\simeq +0.4$ dex. For elements heavier than La, the abundance ratios are consistent with the scaled-solar *r*-process distribution. Below La, the abundances are anomalous when compared to the scaled-solar *s*-process or *r*-process distributions. For these elements, the abundance signature in M62 is in agreement with predictions of the *s*-process from fast-rotating massive stars, although the high [Rb/Y] ratio we measure may be a challenge to this scenario.

Key words: stars: abundances – Galaxy: abundances – globular clusters: individual: NGC 6266.

1 INTRODUCTION

A small, but growing, number of Galactic globular clusters exhibit a star-to-star variation in the relative abundances of the heavy elements. ω Centauri is the most well-known member of this group with its stars spanning a range in metallicity[1] from [Fe/H] $\simeq -2.0$ to [Fe/H] $\simeq -0.5$; for certain elements, the abundance ratios with respect to iron, [X/Fe], exhibit considerable variations with metallicity (e.g. Norris & Da Costa 1995; Smith et al. 2000; Johnson & Pilachowski 2010; D'Orazi et al. 2011). As the most massive Galactic globular cluster and in light of its complex chemical enrichment history, ω Cen is regarded to be the core of a disrupted dwarf galaxy (e.g. Freeman 1993; Bekki & Freeman 2003; Bekki & Norris 2006).

★Based in part on data collected at Subaru Telescope, which is operated by the National Astronomical Observatory of Japan. This paper includes data gathered with the 6.5 metre Magellan Telescopes located at Las Campanas Observatory, Chile.

† E-mail: yong@mso.anu.edu.au
‡ Stromlo Fellow.

[1] Here and throughout the paper, iron is the canonical measure of metallicity and we adopt the standard spectroscopic notation [Fe/H] = $\log_{10}(N_{\rm Fe}/N_{\rm H})_\star - \log_{10}(N_{\rm Fe}/N_{\rm H})_\odot$.

Table 1. Program stars, radial velocities and stellar parameters.

Name[a]	RA 2000	Dec. 2000	J^b	H^b	K^b	RV (km s^{-1})	σRV[c] (km s^{-1})	$T_{\rm eff}$ (K)	log g (cm s^{-2})	ξ_t (km s^{-1})	[m/H] (dex)	[Fe/H] (dex)
(1)	(2)	(3)	(4)	(5)	(6)	(7)	(8)	(9)	(10)	(11)	(12)	(13)
Subaru Telescope Observations 2013 07 17												
A5	17 01 16.21	−30 03 31.81	9.782	8.847	8.583	−75.0	0.2	3950	0.50	1.79	−1.10	−1.12
A7	17 01 17.50	−30 03 20.60	9.602	8.608	8.389	−89.3	0.5	3925	0.20	1.89	−1.10	−1.15
A14	17 01 17.29	−30 03 58.69	11.476	10.710	10.529	−54.2	0.2	4400	1.40	1.53	−1.10	−1.10
A27	17 01 25.19	−30 04 09.85	11.779	11.124	10.989	−69.9	0.4	4625	1.50	1.76	−1.20	−1.24
A124	17 01 00.28	−30 07 38.28	11.449	10.756	10.536	−68.2	0.3	4450	1.00	1.64	−1.20	−1.19
A195	17 01 12.63	−30 03 40.78	11.988	11.318	11.157	−0.1	0.4	...	...	...	...	...
Magellan Telescope Observations 2012 06 26												
c53	17 01 15.20	−30 08 36.50	10.101	9.246	...	−73.6	0.2	4450	1.40	1.78	−1.10	−1.11
d10	17 01 16.80	−30 08 18.00	10.125	9.145	...	−59.0	0.2	4175	0.90	1.90	−1.10	−1.15

[a]AXXX names are from Alcaino (1978) while c53 and d10 are from Strömgren photometry taken by JA-G.
[b]Photometry for the AXXX stars is from 2MASS (Skrutskie et al. 2006). Photometry for c53 and d10 are from Valenti et al. (2007).
[c]The uncertainties are the standard error of the mean.

M54 is the second most massive Galactic globular cluster. It displays a key characteristic shared by ω Centauri but absent in the majority of clusters, namely, a metallicity dispersion (Carretta et al. 2010a), albeit of smaller amplitude than that found in ω Centauri. That M54 is the nuclear star cluster of the Sagittarius dwarf spheroidal galaxy lends further support to the hypothesis that massive globular clusters with metallicity variations may be the nuclei of disrupted dwarf galaxies (although Bellazzini et al. 2008 argue that the nucleus of Sgr likely formed independently of M54). When considering the ensemble of globular clusters with unusual chemical abundance ratios[2] (dispersions in metallicity and/or neutron-capture elements), it is clear that these objects are preferentially the more luminous, and therefore the more massive, clusters.

Lee, Gim & Casetti-Dinescu (2007) considered globular clusters with an extended horizontal branch (i.e. a horizontal branch with extremely blue stars) which likely signifies the presence of He abundance variations (D'Antona et al. 2002). They argued that not only are clusters with an extended horizontal branch preferentially more massive, but also when considered together the clusters have different kinematics from other groupings of the Galactic globular cluster population. The sample of clusters with extended horizontal branches includes ω Cen, M54 and M22, all of which exhibit metallicity variations. Lee et al. (2007) showed that such clusters had kinematics consistent with accretion and thus likely have a different origin to the bulk of the cluster population.

The identification of additional globular clusters with peculiar chemical abundance patterns (e.g. star-to-star variations in metallicity) would advance our understanding of the range and relative frequency of the abundance spread phenomenon in the Galactic globular cluster system. Additionally, quantifying the number of accreted systems has important consequences for understanding the formation and evolution of our Galaxy (Freeman & Bland-Hawthorn 2002). To this end, the most obvious objects to study are the most massive globular clusters with extended horizontal branches. M62 (NGC 6266) is the ninth most luminous cluster (Harris 1996) and has an extended blue horizontal branch. In the F439W − F555W versus F555W colour–magnitude diagram (CMD) presented by Piotto et al. (2002), the horizontal branch extends down in luminosity to the main-sequence turn-off. The extended horizontal branch is also readily identified in dereddened V versus $B-V$ and V versus $V-I$ diagrams (Alonso-García et al. 2011, 2012). M62 ranks fifth in the number of millisecond pulsars (Cocozza et al. 2008), and there may be a connection between multiple stellar populations and the numbers of millisecond pulsars (Lanzoni et al. 2010). Contreras et al. (2010) find that M62 could contain the most RR-Lyrae of any Galactic globular cluster and is a typical Oosterhoff type I system. This cluster lies in the vicinity of the bulge, although proper-motion measurements indicate that it probably belongs to the thick disc (Dinescu et al. 2003). M62 is highly reddened, $E(B-V)=0.47$ (Harris 1996), and it is severely affected by differential reddening, $\Delta E(B-V)\sim 0.25$ (Alonso-García et al. 2012).

The goal of the present paper is to conduct a detailed chemical abundance analysis of M62 based on high-resolution, high signal-to-noise ratio (S/N) spectra. To our knowledge this is the first such analysis of this cluster and this work therefore represents an essential step towards completing the census and characterization of the Galaxy's most massive globular clusters.

2 OBSERVATIONS AND ANALYSIS

2.1 Target selection and spectroscopic observations

Six targets were selected from Rutledge et al. (1997) (see Table 1). All were high probability members based on the published radial velocities and were observed with the High Dispersion Spectrograph (HDS; Noguchi et al. 2002) on the Subaru Telescope on 2013 July 17. The exposure times ranged from 16 to 40 min per program star. We used the StdYb setting and the 0.8 arcsec slit which resulted in a wavelength coverage from ∼4100 to ∼6800 Å at a spectral resolution of $R=45\,000$. There were approximately four pixels per resolution element. Spectra of a telluric standard (HD 163955) and a radial velocity standard (HD 182572) were also taken during this observing run.

[2] In addition to ω Cen and M54, the other clusters include M15 (Sneden et al. 2000; Otsuki et al. 2006; Sobeck et al. 2011; Worley et al. 2013), NGC 362 (Carretta et al. 2013), NGC 1851 (Yong & Grundahl 2008; Villanova, Geisler & Piotto 2010; Carretta et al. 2011), NGC 2419 (Cohen et al. 2010; Cohen, Huang & Kirby 2011; Cohen & Kirby 2012; Mucciarelli et al. 2012), NGC 3201 (Simmerer et al. 2013), NGC 5824 (Saviane et al. 2012), NGC 6656 (Da Costa et al. 2009; Da Costa & Marino 2011; Marino et al. 2009, 2011; Roederer, Marino & Sneden 2011; Alves-Brito et al. 2012), NGC 7089 (Lardo et al. 2012, 2013) and Terzan 5 (Ferraro et al. 2009; Origlia et al. 2011, 2013).

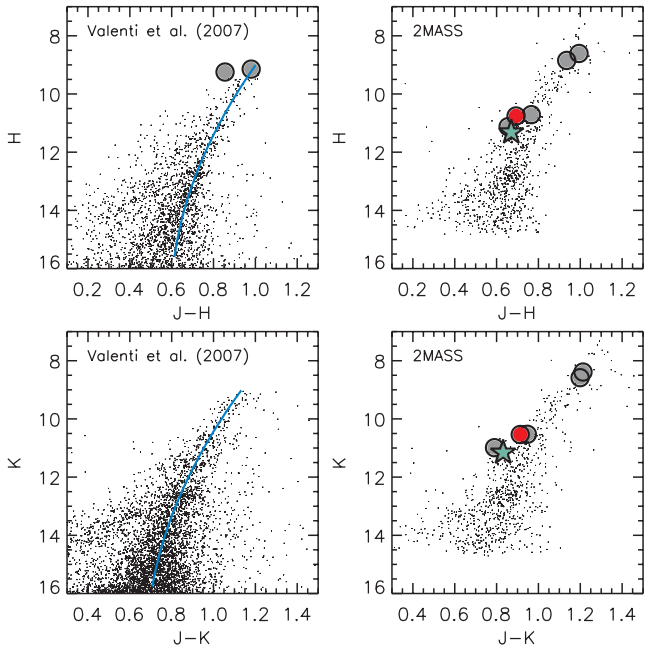

Figure 1. *JHK* colour–magnitude diagrams for M62 from Valenti et al. (2007) (left panels) and 2MASS Skrutskie et al. (2006) (right panels; taking only objects within a radius of 3.5 arcmin and 'AAA' photometric quality flags). The aqua star represents the radial velocity non-member, star A195, and the red circle represents star A124, the possible non-member based on chemical abundances. All other program stars are shown as grey circles. In the left panels, the solid line represents the mean RGB ridge line from Valenti et al. (2007).

Two additional targets were selected from Strömgren photometry obtained by J.A-G and observed using the MIKE spectrograph (Bernstein et al. 2003) at the Magellan-II Telescope on 2012 June 26. The exposure times were 1 h for each star. The 0.7 arcsec slit was employed providing a spectral resolution of $R = 35\,000$ (blue CCD) and $R = 27\,000$ (red CCD) with a wavelength coverage from ∼3800 to ∼9000 Å. There were approximately four pixels per resolution element. A telluric standard (HD 170642) was also observed.

In Fig. 1, we show the locations of our targets in *JHK* CMD. The photometry is from Valenti, Ferraro & Origlia (2007) and 2MASS (Skrutskie et al. 2006).

2.2 Data reduction and analysis

The Subaru spectra were reduced using IRAF.[3] The Magellan spectra were reduced using a combination of IRAF and the MTOOLS package.[4] In both cases, the approach was similar to that described in Yong et al. (2006). In Fig. 2, we plot a region of the spectra for the program stars. The telluric standards were used to correct regions affected by telluric absorption. Star A195 had a S/N = 40 per pixel near 6000 Å. Excluding this star, the S/N ranged from S/N = 65 per pixel (stars A14 and A27) to S/N = 110 per pixel (star d10).

For the program stars observed with Subaru, heliocentric radial velocities were measured by cross-correlating each star against the

[3] IRAF is distributed by the National Optical Astronomy Observatories, which are operated by the Association of Universities for Research in Astronomy, Inc., under cooperative agreement with the National Science Foundation.
[4] www.lco.cl/telescopes-information/magellan/instruments/mike/iraf-tools/iraf-mtools-package

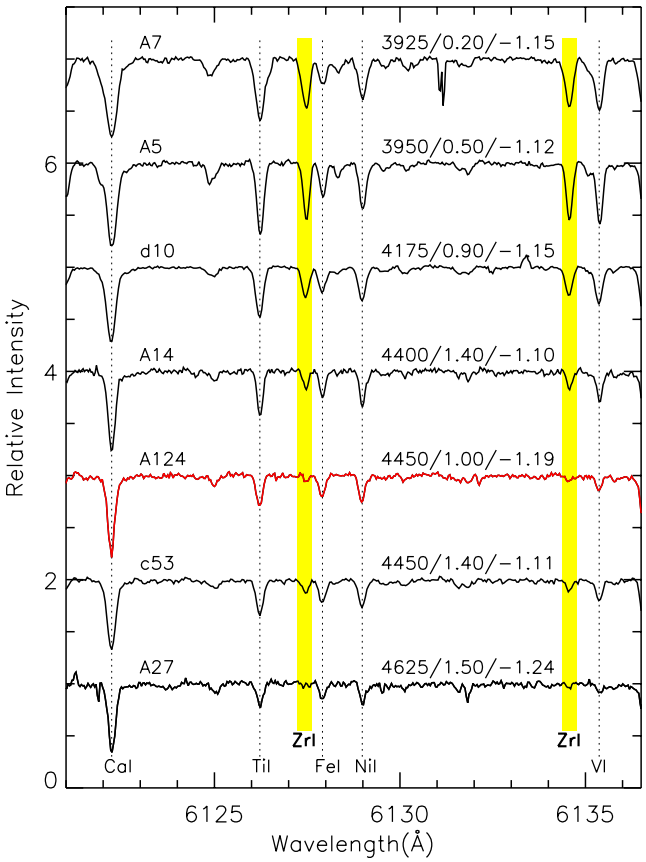

Figure 2. A portion of the spectra for the program stars. The yellow region highlights two Zr lines used in the analysis. The positions of other atomic lines and the stellar parameters ($T_{\rm eff}$/log g/[Fe/H]) are included. The red spectrum is star A124, a possible non-member based on the chemical abundances.

radial velocity standard, HD 182572, for which we adopted a value[5] of −100.35 km s^{-1}. For the program stars observed with Magellan, the radial velocities were determined by measuring the positions of a large number (several hundred) of atomic absorption features. The radial velocities are presented in Table 1 and we note that star A195 is not a radial velocity member.

Equivalent widths (EW) were measured using routines in IRAF and DAOSPEC (Stetson & Pancino 2008). We note that every line measured using DAOSPEC was also measured, and visually inspected, using IRAF. For all stars, there was good agreement between the two sets of measurements; for a given star, the average difference in EWs between IRAF and DAOSPEC was 0.1 mÅ with a dispersion of 3 mÅ. The line list and EW measurements (average of IRAF and DAOSPEC) are presented in Table 2.

The stellar parameters were determined using a traditional spectroscopic approach. One-dimensional local thermodynamic equilibrium (LTE) model atmospheres were taken from the Castelli & Kurucz (2003) alpha enhanced, [α/Fe] = +0.4, grid. To produce particular models we used the interpolation software tested in Allende Prieto et al. (2004). Chemical abundances were generated using the LTE stellar line analysis program MOOG (Sneden 1973; Sobeck et al. 2011). The effective temperature, $T_{\rm eff}$, was obtained when there was no trend between the abundance from Fe I lines and the lower excitation potential. The surface gravity, log g, was

[5] obswww.unige.ch/∼udry/std/stdnew.dat

Table 2. Line list and EWs.

Wavelength Å (1)	Species[a] (2)	L.E.P (eV) (3)	log *gf* (4)	A5 (mÅ) (5)	A7 (mÅ) (6)	A14 (mÅ) (7)	A27 (mÅ) (8)	A124 (mÅ) (9)	c53 (mÅ) (10)	d10 (mÅ) (11)	Source[b] (12)
6300.31	8.0	0.00	−9.75	33.0	48.9	<15.0	67.0	48.8	<15.0	60.2	B
6363.78	8.0	0.02	−10.25	...	17.0	...	21.2	22.1	...	34.4	A
7771.95	8.0	9.15	0.35	...	...	...	...	...	...	12.8	B
7774.18	8.0	9.15	0.21	...	...	...	...	...	...	10.1	B
5682.65	11.0	2.10	−0.67	...	...	114.8	51.2	...	110.3	98.0	B

[a]The digits to the left of the decimal point are the atomic number. The digit to the right of the decimal point is the ionization state (0 = neutral, 1 = singly ionized).

[b]A = log *gf* values taken from Yong et al. (2005) where the references include Den Hartog et al. (2003), Ivans et al. (2001), Kurucz & Bell (1995), Prochaska et al. (2000), Ramírez & Cohen (2002); B = Gratton et al. (2003); C = Oxford group including Blackwell et al. (1979a, 1980, 1986), Blackwell, Petford & Shallis (1979b), Blackwell, Lynas-Gray & Smith (1995); D = Biemont et al. (1991); E1 = Fuhr & Wiese (2009), E2 = Roederer & Lawler (2012), E3 = Biémont et al. (2011), E4 = Biemont et al. (1981), E5 = Lawler, Bonvallet & Sneden (2001a), E6 = Lawler et al. (2009), E7 = Li et al. (2007), E8 = Den Hartog et al. (2003), E9 = Lawler et al. (2006), E10 = Lawler et al. (2001b), E11 = Roederer et al. (2012); F = Lambert & Luck (1976).

Note. This table is published in its entirety in the electronic edition of the paper. A portion is shown here for guidance regarding its form and content.

established by forcing the iron abundance derived from Fe I and Fe II lines to be equal. The microturbulent velocity, ξ_t, was adjusted until the abundance from Fe I lines exhibited no trend with reduced EW, log (EW/λ). Finally, we required the derived metallicity to be within 0.1 dex of the value adopted in the model atmosphere. The final stellar parameters (see Table 1) were established only when all conditions above were simultaneously satisfied. The uncertainties in $T_{\rm eff}$, log g and ξ_t are estimated to be 50 K, 0.20 dex and 0.20 km s^{-1}, respectively. We do not present results for star A195 since it is not a radial velocity member and our preliminary analysis indicated that it is a super-solar metallicity clump giant ($T_{\rm eff} = 4750$, log g = 3.1, [Fe/H] = +0.17).

Chemical abundances were determined using the final model atmosphere, measured EW and MOOG. For Cu and the neutron-capture elements, abundances were determined via spectrum synthesis. Lines affected by hyperfine splitting (HFS) and/or isotope shifts (e.g. Sc II, V I, Mn I, Co I, Rb I, Ba II, La II, Pr II, Eu II and Pb I) were treated appropriately using the HFS data from Kurucz & Bell (1995) or other sources as noted in Table 2. For Rb and Pb, the wavelength coverage necessary to measure these elements was only obtained in the two stars observed with Magellan (see Figs 3 and 4). C abundances were determined from spectrum synthesis of the 4300 Å CH molecular lines using the CH line list compiled by Plez et al. (2009, private communication). In our analysis, the dissociation energy for CH was 3.465 eV. The Asplund et al. (2009) solar abundances were adopted and the chemical abundances are presented in Table 3.

The uncertainties in the chemical abundances were obtained in the following manner. We repeated the analysis and varied the stellar parameters, one at a time, by their uncertainties. We also considered the uncertainty of the metallicity used to generate the model atmosphere, [M/H], and adjusted this value by +0.2 dex. The systematic error was determined by adding these four error terms in quadrature, and we assume these values are symmetric for positive and negative changes. Following Norris et al. (2010), the random error (s.e.$_{\log\epsilon}$) was obtained by taking max(s.e.$_{\log\epsilon}$, 0.20/$\sqrt{N_{\rm lines}}$). The second term is what would be expected for a set of $N_{\rm lines}$ with a dispersion of 0.20 dex (a conservative value based on the abundance dispersion exhibited by Fe I lines). By adding the systematic and random errors, in quadrature, we obtain the total error which is presented in Table 3.

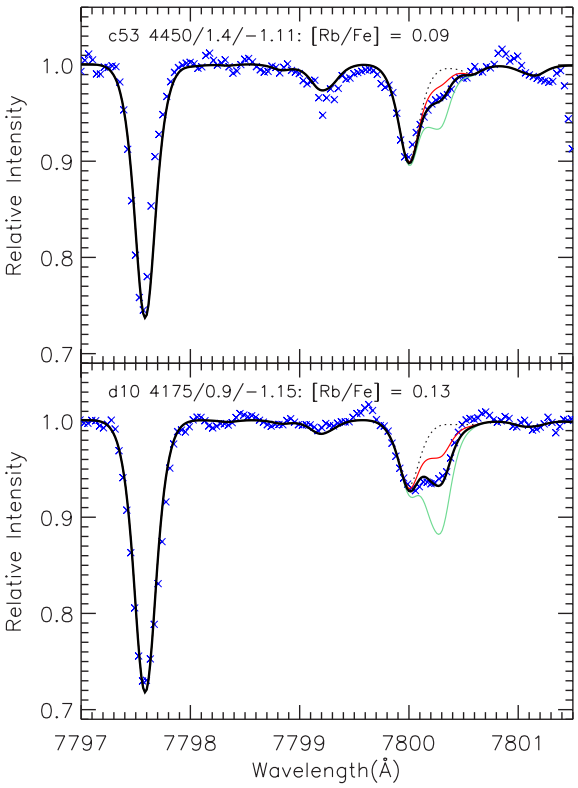

Figure 3. Observed and synthetic spectra for stars c53 (upper) and d10 (lower) near the 7800 Å Rb feature. The thick black line represents the best fit, thin red and green lines are Δ[Rb/Fe] = ±0.3 dex from the line of best fit and the dotted line has no Rb. The stellar parameters ($T_{\rm eff}$/log g/[Fe/H]) and [Rb/Fe] abundance are included in each panel.

3 RESULTS

3.1 Cluster membership and radial velocities

With the exception of star A195, all program stars have radial velocities consistent with cluster membership. According to the Harris (1996) catalogue, M62 has a heliocentric radial velocity of −70.1 ± 1.4 km s^{-1} and a central velocity dispersion of 14.3 ± 0.4 km s^{-1}.

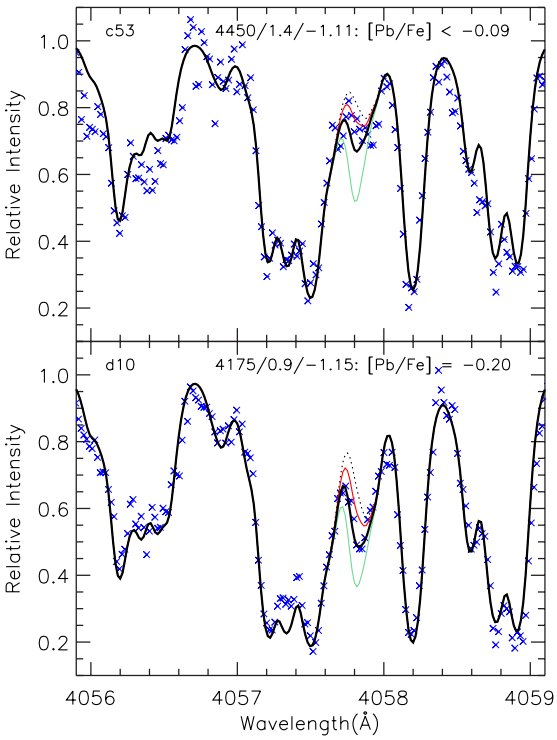

Figure 4. Observed and synthetic spectra for stars c53 (upper) and d10 (lower) near the 4058 Å Pb feature. The thick black line represents the best fit (d10) or abundance limit (c53), thin red and green lines are Δ[Pb/Fe] = ±0.5 dex from the line of best fit and the dotted line has no Pb. The stellar parameters ($T_{\rm eff}$/log g/[Fe/H]) and [Pb/Fe] abundance are included in each panel.

Table 3. Chemical abundances for the program stars.

Name	A(X)	$N_{\rm lines}$	s.e.$_{\log\epsilon}$	[X/Fe]	Total error
		C from CH			
A5	6.46	synth	...	−0.85	0.21
A7	6.31	synth	...	−0.97	0.23
A14	6.41	synth	...	−0.92	0.21
A27	6.76	synth	...	−0.43	0.22
A124	6.76	synth	...	−0.48	0.23
c53	6.71	synth	...	−0.61	0.22
d10	7.01	synth	...	−0.27	0.22
		O I			
A5	7.79	2	0.07	0.30	0.18
A7	7.79	2	0.04	0.39	0.20
A14	7.68	1	...	<0.16	...
A27	8.40	2	0.09	1.05	0.18
A124	8.08	2	0.03	0.68	0.18
c53	7.66	1	...	<0.17	...
d10	8.31	4	0.04	0.89	0.14
		Na I			
A5	5.67	2	0.04	0.64	0.18
A7	5.63	2	0.00	0.68	0.17
A14	5.79	3	0.04	0.72	0.13
A27	4.87	3	0.05	−0.04	0.13
A124	4.86	2	0.01	−0.09	0.15
c53	5.59	3	0.06	0.55	0.12
d10	5.18	4	0.04	0.21	0.12

Note. This table is published in its entirety in the electronic edition of the paper. A portion is shown here for guidance regarding its form and content.

For our seven program stars, we find an average heliocentric radial velocity of −69.9 ± 4.3 km s^{-1} (σ = 11.4 km s^{-1}).

As we shall discuss in the following subsection, star A124 has low abundance ratios for the neutron-capture elements compared to the other program stars and so the possibility exists that this object may not be a cluster member. With a radial velocity of −68.2 ± 0.3 km s^{-1}, excluding this star would not substantially change the mean radial velocity and velocity dispersion we measure for this cluster.

To investigate the likelihood of observing field stars in the vicinity of M62 with stellar parameters ($T_{\rm eff}$, log g and [Fe/H]) and radial velocities comparable to the program stars, we make use of the Besançon model (Robin et al. 2003). First, we consider all stars within a one square degree field centred on M62. Secondly, we restricted the sample to lie near the RGB in the K versus $J-K$ CMD; specifically, the left edge was defined as the line from ($J-K$, K) = (0.55,12.0) to ($J-K$, K) = (1.1,8.0) and the right edge as the line from ($J-K$, K) = (1.05,12.0) to ($J-K$, K) = (1.4,8.0). We find 13 281 such stars from the Besançon model. Thirdly, of these 13 281 stars we counted the number that satisfied the following constraints: (*i*) −95 ≤ RV ≤ −45 km s^{-1} and (*ii*) −1.35 ≤ [Fe/H] ≤ −1.00 dex. And finally, we counted the numbers of stars that lay in a particular region in the $T_{\rm eff}$-log g plane, specifically, the area is bounded at the left edge by the line from ($T_{\rm eff}$,log g) = (4925,2.0) to ($T_{\rm eff}$,log g) = (4225,0.0), at the right edge by the line from ($T_{\rm eff}$,log g) = (4200,2.0) to ($T_{\rm eff}$,log g) = (3625,0.0) both with 0.0 ≤ log g ≤ 2.0. We found 490 stars in the Besançon model that satisfied all criteria and therefore estimate that given a sample of stars occupying similar locations in *JHK* CMDs as the program stars, the probability of observing a field star with stellar parameters and a radial velocity consistent with the program stars is roughly 4 per cent. In our sample of seven stars, having one field star with stellar parameters and a radial velocity consistent with the cluster sample is not unreasonable given the small number statistics. Accurate proper-motion and parallax measurements from *GAIA* would establish cluster membership, or otherwise, for this object.

3.2 Chemical abundances

For the program stars, we measure a mean metallicity of [Fe/H] = −1.15 ± 0.02 (σ = 0.05). Our metallicity is consistent with previous measurements based primarily on low-resolution spectroscopic measurements: [Fe/H] = −1.28 ± 0.15 (Zinn & West 1984); [Fe/H] = −1.02 ± 0.04 (Carretta & Gratton 1997); [Fe/H] = −1.19 (Kraft & Ivans 2003) when using MARCS model atmospheres (Gustafsson et al. 1975); [Fe/H] = −1.18 ± 0.07 (Carretta et al. 2009). The dispersion in [Fe/H] based on our program stars can be entirely attributed to the measurement uncertainty. The mean metallicity and dispersion are essentially unchanged if we exclude the 'neutron-capture poor' star A124 with [Fe/H] = −1.19.

For the light elements, we find evidence for a star-to-star variation for C, O, Na and Al and perhaps Mg (see Fig. 5). For O, Na and Al, the observed abundance dispersion exceeds the average measurement error by a factor of ∼2 indicating a genuine abundance spread for these elements. These abundance dispersions are confirmed by the statistical significance of the correlations between the following pairs of elements, $\gtrsim 3\sigma$ for [O/Fe] versus [Na/Fe] and [Na/Fe] versus [Al/Fe]. There is a suggestion that Mg and Al are anticorrelated, a characteristic found in other, but not all, globular clusters. There is no evidence for an abundance variation for Si, nor for correlations between Si and all other elements as seen in NGC 6752 (Yong et al. 2013).

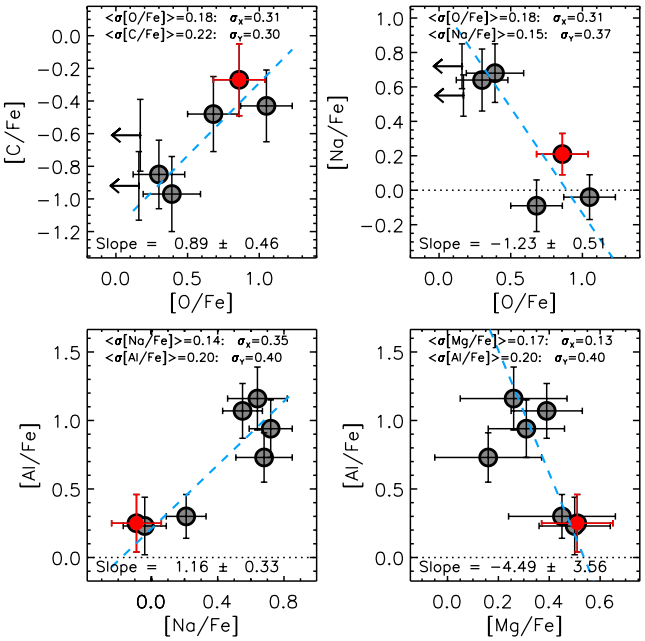

Figure 5. Abundance ratios for combinations of the light elements (C, O, Na, Mg and Al). The red data point is star A124, which has low neutron-capture element abundance ratios compared to the remaining program stars. The dashed line is the linear fit to the data (slope and error are included). The average error ($\langle\sigma$[X/Fe]$\rangle$) and dispersion (σ) in the x-direction and y-direction are included.

In Fig. 6 we plot Ni and a selection of neutron-capture elements versus Na. Star A124, marked in red in this and other figures, exhibits systematically lower abundance ratios for the neutron-capture elements compared to the remaining program stars. For a given element, we can compare the [X/Fe] ratio for star A124 to the average [X/Fe] ratio for the other stars. When doing this for the neutron-capture elements from Sr to Eu for A124, we find an average difference of 0.29 ± 0.02 (σ = 0.07). This difference is approximately twice the average error and suggests that this star is chemically different from the other six program stars, at least for the neutron-capture elements. Thus, our quantitative analysis confirms the visual impression from Fig. 2 in which star A124 has weaker Zr lines relative to other program stars of comparable stellar parameters. Aside from star A124, we find no compelling evidence for an abundance dispersion for the neutron-capture elements. In all cases, the observed abundance dispersion is consistent with the measurement uncertainty. We find no evidence for a statistically significant correlation between any of the heavy elements and Na; such a correlation has been identified in the globular cluster NGC 6752 (Yong et al. 2013).

In Fig. 7, we compare the measured abundance dispersion (including star A124) with the average total error. As already noted, the light elements O, Na and Al exhibit significantly larger dispersions than expected given the measurement uncertainty. For all other elements, with the possible exception of C, the observed abundance dispersions can be attributed to the measurement uncertainty. Note that the abundances for Fe II were forced to match those of Fe I, and this species is not included in Fig. 7. Had we excluded star A124 when generating this figure, the σ(observed) values would have decreased such that a larger proportion of the data would lie below the 1:1 relation. As such, our measurement uncertainties might be overestimated.

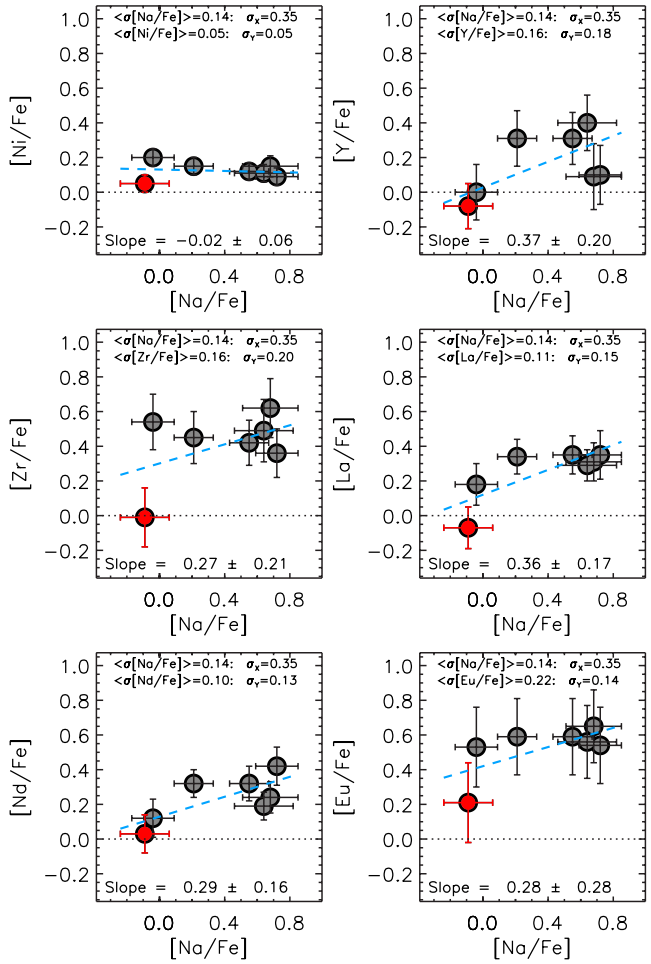

Figure 6. Same as Fig. 5 but for Ni and the neutron-capture elements versus Na.

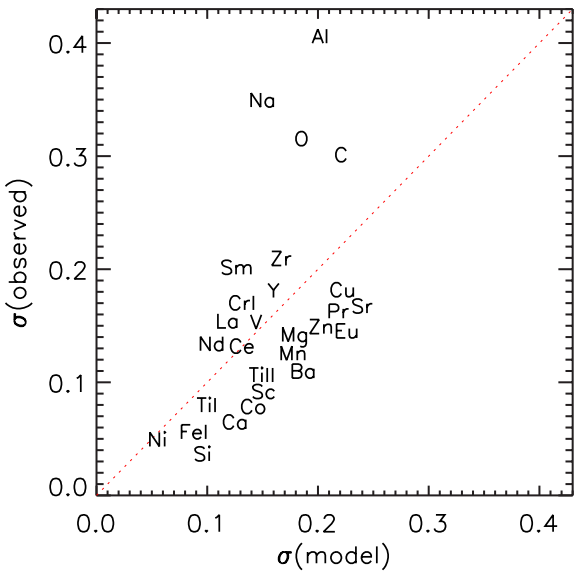

Figure 7. Measured abundance dispersion, σ(observed, including star A124) versus average measurement error, σ(model). The dotted red line is the 1:1 relation. Fe II is not included (see text for details). For clarity, some values have been shifted by up to 0.01 dex.

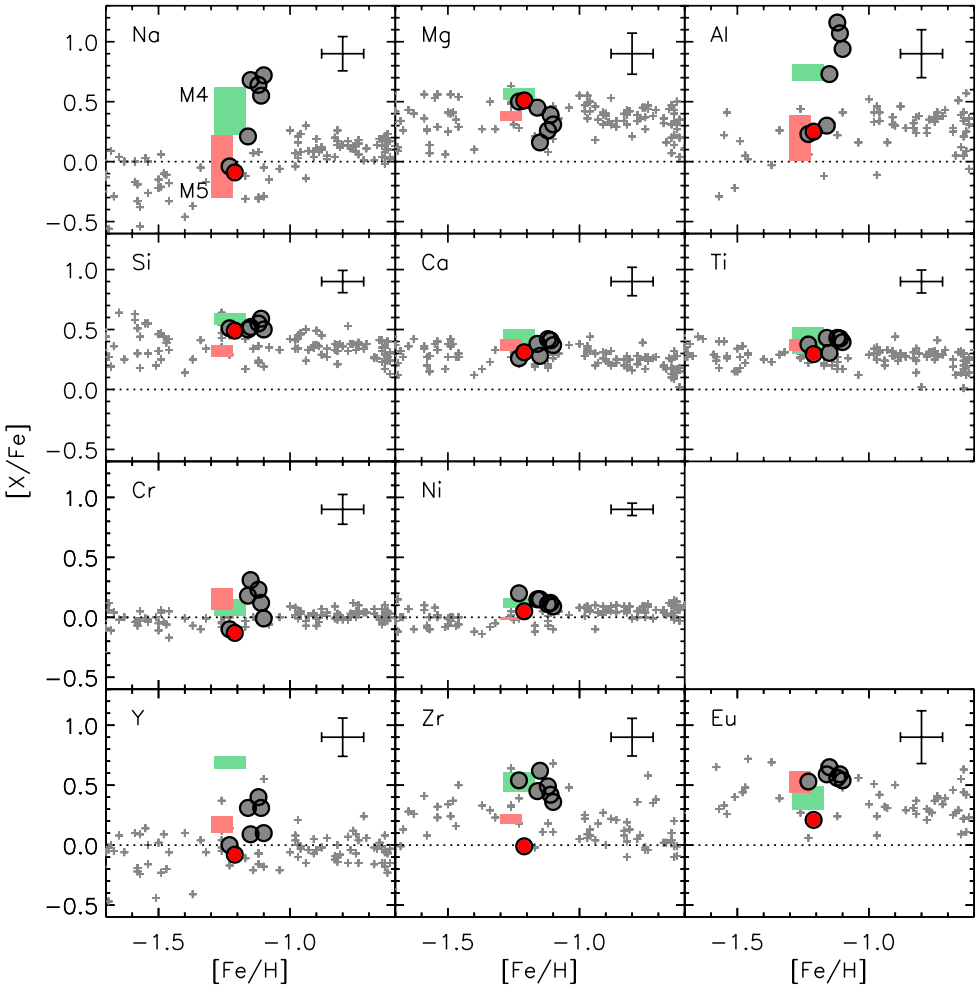

Figure 8. Abundance ratios [X/Fe] versus [Fe/H] for the program stars (the red circle is star A124 with low neutron-capture elements ratios). For Ti, we adopt the average of Ti I and Ti II. A representative error bar is included in each panel. The small grey symbols are field halo stars taken from Fulbright (2000). The shaded aqua and pink regions represent the data (mean value ± standard deviation) for M4 and M5, respectively, taken from Yong et al. (2008a,b).

In Fig. 8, we plot [X/Fe] versus [Fe/H] for the program stars and field stars from Fulbright (2000). For Na and Al, one can clearly see that the abundance dispersions for [Na/Fe] and [Al/Fe] in M62 far exceed that of the field stars of comparable metallicity and that the lower envelope of the cluster values are in good agreement with field stars. Such results have been well established for other clusters (e.g. see reviews by Kraft 1994; Gratton, Sneden & Carretta 2004; Gratton, Carretta & Bragaglia 2012). We note that star A124 has Na and Al abundances in agreement with field stars. Further, the neutron-capture element abundances for this star, while lower than the cluster average, appear typical for field halo stars at the same metallicity, which is consistent with it being a field interloper.

For Si, Ca, Ti, Cr and Ni, the abundance ratios for M62 are in good agreement with field stars of the same metallicity. In Solar system material, elements mainly produced via the *s*-process include Y and Zr, and we refer to these as *s*-process elements. Similarly, elements predominantly produced via the *r*-process in Solar system material are referred to as *r*-process elements and include Eu. For the *s*-process elements Y and Zr, the M62 values lie slightly above field halo stars of comparable metallicity. For the *r*-process element Eu, the M62 values lie near the upper envelope defined by the field stars. (We caution that zero-point offsets may reduce, or amplify, the abundance differences between M62 and the field stars.)

In Fig. 8, we also include the comparable metallicity globular clusters M4 ([Fe/H] = −1.08; Ivans et al. 1999) and M5 ([Fe/H] = −1.21; Ivans et al. 2001) using the data from Yong et al. (2008a,b). For Na and Al, while the abundance dispersions found in M4 and M5 are considerably smaller than in M62, we note that our sample sizes are small. Examination of the larger samples in Ivans et al. (1999, 2001) and Marino et al. (2008) also indicates that the abundance dispersions for Na and Al in M4 and M5 are probably smaller than those of M62. For the elements Si to Ni, the abundance ratios [X/Fe] in M4 and M5 match those of M62 and field stars in their metallicity range. For the *s*-process elements, M4 is known to have larger [X/Fe] ratios than M5.

We conclude this section by noting some physical parameters for M4, M5 and M62 which may provide insight into any chemical abundance differences between these clusters. De Angeli et al. (2005) measured relative ages for these three clusters and found M5 to be 10–15 per cent younger[6] than M4 and M62 with the latter two being coeval. Marín-Franch et al. (2009) also found M5 to be slightly younger than M4. On the other hand, VandenBerg

[6] De Angeli et al. (2005) regard their typical uncertainties to be 5 to 8 per cent.

et al. (2013) measured ages for M4 and M5 of 11.50 Gyr, but did not study M62. The absolute luminosities for M4, M5 and M62 are −7.19, −8.81 and −9.18, respectively, and the central velocity dispersions are 4.0, 5.5 and 14.3 km s^{-1}, respectively (Harris 1996). M4 and M62 have orbits that are restricted to the inner disc and bulge, apocentric radii of $R_a = 5.9$ kpc (Dinescu, Girard & van Altena 1999) and $R_a = 3.1$ kpc (Allen, Moreno & Pichardo 2006), respectively while M5 has an orbit which may be consistent with an accretion event, $R_a = 35.4$ kpc.

4 DISCUSSION

The focus of this discussion is to examine the nature of M62 in light of its chemical abundances. In Table 4, we present the average cluster abundance ratios with and without star A124, which has lower neutron-capture element abundances.

4.1 The light elements

It is now well established that every globular cluster exhibits star-to-star abundance variations for C, N, O, F, Na, Mg and Al (e.g. see reviews by Kraft 1994; Gratton et al. 2012). These abundance variations are believed to have been produced via hydrogen-burning at high temperature in asymptotic giant branch (AGB) stars, fast-rotating massive stars and/or massive binaries (e.g. Fenner et al. 2004; Ventura & D'Antona 2005; Decressin et al. 2007; de Mink et al. 2009; Marcolini et al. 2009).

Table 4. Mean abundances and abundance dispersions for the program stars (excluding abundance limits).

Species	Z	[X/Fe]	σ[X/Fe][a]	[X/Fe]	σ[X/Fe][a]
		All stars		Excluding A124	
O I	8	0.52	0.35	0.49	0.38
Na I	11	0.38	0.35	0.46	0.31
Mg I	12	0.37	0.13	0.34	0.13
Al I	13	0.67	0.40	0.74	0.39
Si I	14	0.52	0.04	0.53	0.04
Ca I	20	0.35	0.06	0.35	0.07
Sc II	21	0.20	0.09	0.23	0.06
Ti I	22	0.34	0.08	0.36	0.06
Ti II	22	0.42	0.09	0.43	0.10
V I	23	0.22	0.15	0.27	0.11
Cr I	24	0.09	0.17	0.12	0.15
Mn I	25	−0.30	0.12	−0.30	0.13
Fe I[b]	26	−1.15	0.05	−1.15	0.05
Fe II[b]	26	−1.16	0.05	−1.15	0.05
Co I	27	0.08	0.08	0.09	0.08
Ni I	28	0.12	0.05	0.14	0.04
Cu I	29	−0.22	0.18	−0.19	0.17
Zn I	30	0.11	0.15	0.10	0.16
Rb I[c]	37	0.11	0.03	0.11	0.03
Sr I	38	−0.39	0.17	−0.33	0.08
Y II	39	0.16	0.18	0.20	0.16
Zr I	40	0.41	0.20	0.48	0.09
Ba II	56	0.32	0.11	0.36	0.03
La II	57	0.25	0.15	0.30	0.07
Ce II	58	−0.01	0.13	0.04	0.07
Pr II	59	0.18	0.15	0.23	0.09
Nd II	60	0.23	0.13	0.27	0.11
Sm II	62	0.32	0.20	0.37	0.14
Eu II	63	0.52	0.14	0.58	0.04
Pb I[c]	82	−0.20	...	−0.20	...

[a] Standard deviation.
[b] [Fe I/H] or [Fe II/H].
[c] Measurements only for stars c53 and d10.

Carretta (2006) and Carretta et al. (2010b) found that the abundance dispersions for the light elements correlate with various physical parameters. In particular, they noted that the interquartile range (IQR) for [O/Fe], [Na/Fe], [O/Na] and [Mg/Al] exhibits a correlation with the absolute luminosity, i.e. total mass. Within our modest sample, assuming for the purposes of this exercise that the [O/Fe] limits are detections, we find IQR[O/Na] = 1.11 and IQR[Mg/Al] = 0.89. With $M_V = -9.18$ (Harris 1996), the IQR values for M62 are consistent with those of other luminous clusters.

4.2 The neutron-capture elements

In Fig. 9 we plot [X/Fe] versus atomic number for M62, M4 and M5. Regarding the *s*-process elements, Zr, Ba and La have ratios of [X/Fe] $\simeq +0.4$. Such values differ from the majority of field halo stars of similar metallicity and from the comparable metallicity globular cluster M5. On the other hand, these abundance ratios in M62 are comparable (but not identical) to M4, a cluster believed to have formed from gas enriched in *s*-process material. It is intriguing that both M4 and M62 are inner disc globular clusters of similar metallicity. Enhancements in the *s*-process elements are also seen in the globular clusters ω Cen and M22 (e.g. Da Costa & Marino 2011, and references therein). For elements other than Zr, Ba and La, the abundance pattern in M62 more closely resembles that of M5 rather than M4.

At the metallicity of these clusters, published neutron-capture element abundances in inner disc and bulge stars are limited. The Fulbright (2000) comparison field stars in Fig. 8 are solar neighbourhood objects. Since the pioneering work by McWilliam & Rich (1994) on chemical abundances in the bulge, the handful of papers presenting neutron-capture element abundances at or below [Fe/H] = −1.0 in the inner disc or bulge include Johnson et al. (2012) and Bensby et al. (2013). Although their sample sizes are modest, some stars are enriched with material produced by *s*-process nucleosynthesis. Among the bulge and inner disc globular clusters with [Fe/H] $\lesssim -1.0$, NGC 6522 exhibits enhancements in the *s*-process elements (Barbuy et al. 2009; Chiappini et al. 2011) while HP-1 (Barbuy et al. 2006) and NGC 6558 (Barbuy et al. 2007) do not.

The abundances of Rb and Pb offer important diagnostics regarding the nature of the *s*-process. Due to a branching point at ^{85}Kr along the *s*-process path, the Rb/Zr ratio is sensitive to the neutron density at the site of the *s*-process. At high neutron density, the [Rb/Zr] ratio is expected to be a factor of ∼10 larger than at low neutron density (Beer & Macklin 1989; Kappeler, Beer & Wisshak 1989), although the yields depend on details in the models and nuclear reaction rates (Pignatari et al. 2008, 2010; van Raai et al. 2012). Indeed, large Rb abundances have been observed in massive AGB stars (García-Hernández et al. 2006, 2009). Pb and Bi are the last stable nuclei along the *s*-process path. If the total neutron exposure, or neutron supply per seed nuclei, is sufficiently high, large overabundances of these elements are predicted (e.g. Gallino et al. 1998; Busso, Gallino & Wasserburg 1999; Busso et al. 2001; Goriely & Mowlavi 2000), and have been observed (e.g. Van Eck et al. 2001; Ivans et al. 2005).

As already noted, measurements of Rb and Pb were only possible for the two program stars observed at the Magellan Telescope. In Fig. 3 we show observed and synthetic spectra near the 7800 Å Rb I feature. We measure values of [Rb/Fe] = +0.09 and +0.13 for stars c53 and d10, respectively. As can be seen in Fig. 9, those

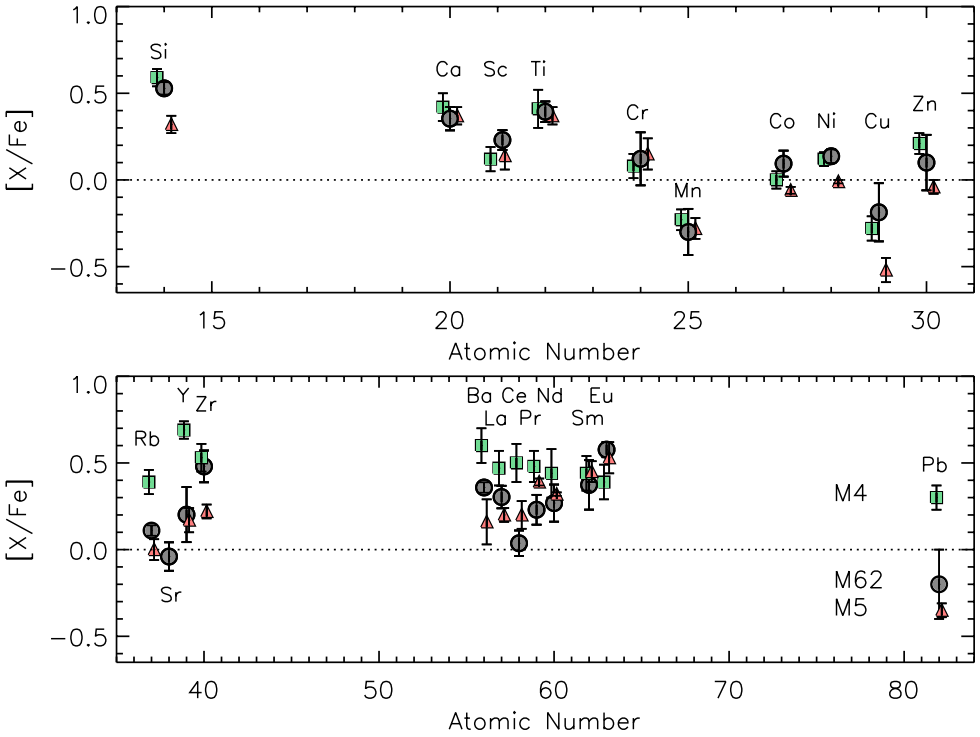

Figure 9. Abundance ratios [X/Fe] versus atomic number for M62 (large grey circles), M4 (small aqua squares) and M5 (small pink triangles). For M62, we exclude star A124. For M4 and M5, the data are from Yong et al. (2008b). For Sr, we apply a non-LTE correction of 0.29 dex (see Section 4.2 for details) and the M4 and M5 Sr values are not plotted since they are derived from a different line than in the present work.

values fall closer to M5 ([Rb/Fe] = 0.00) than to M4 ([Rb/Fe] = +0.39; Yong et al. 2008b). D'Orazi et al. (2013) measured [Rb/Fe] in three globular clusters (NGC 6752, NGC 1904 and 47 Tuc) and found constant values in each cluster at the [Rb/Fe] $\simeq$ 0.0 level. The [Rb/Zr] ratios are −0.04 and −0.05 for stars c53 and d10, respectively, when the Zr abundances are shifted on the Smith et al. (2000) scale as described in Yong et al. (2006). The [Rb/Zr] ratios in M62 lie below those of M4 and M5, [Rb/Zr] = +0.17 and +0.08, respectively, but above the ω Cen values (Smith et al. 2000). In summary, the low [Rb/Fe] and [Rb/Zr] ratios in M62 offer no support for a weak *s*-process contribution [i.e. the *s*-process in massive stars from the ^{22}Ne(α,*n*)^{25}Mg reaction] from which the high neutron density would result in considerably higher [Rb/Fe] and [Rb/Zr] ratios than observed. We will revisit the [Rb/Zr] ratio in the context of fast-rotating massive stars later in this subsection.

The Sr abundance in M62, $\langle$[Sr/Fe]$\rangle$ = −0.39, appears to be unusually low compared to the neighbouring elements, $\langle$[Rb/Fe]$\rangle$ = +0.11 and $\langle$[Y/Fe]$\rangle$ = +0.16. Since our analysis only considered one line, Sr I 4607.33 Å, we regard the low Sr abundance with some caution. Indeed, other studies that consider the 4607.33 Å Sr I line in globular cluster giants find [Sr/Fe] ratios that are lower than for the neighbouring elements [Rb/Fe], [Y/Fe] and [Zr/Fe] (e.g. Roederer et al. 2011; Yong et al., in preparation). Bergemann et al. (2012) investigated non-LTE corrections for the 4607.33 Å Sr line, and for $T_{\rm eff}$/log *g*/[Fe/H] = 4400/2.2/−1.2, the correction is 0.29 dex. The magnitude and sign of this correction would help to reconcile the Sr abundances with those of Rb and Y. In Fig. 9 we adjust the Sr abundance accordingly.

In Fig. 4, we plot observed and synthetic spectra near the 4058 Å Pb I feature. We measure values of [Pb/Fe] < −0.09 and [Pb/Fe] = −0.20 for stars c53 and d10, respectively. For comparison, the average values in M4 and M5 are [Pb/Fe] = +0.30 and −0.35, respectively (Yong et al. 2008b). Thus, the M62 values for [Pb/Fe] lie closer to M5 than to M4 (see Fig. 9). Roederer et al. (2010) argue that the Pb/Eu ratio offers a good diagnostic of the presence of *s*-process enriched material. For M62, the Pb to Eu ratios are at the same level as the (more metal-poor) '*r*-process standard stars' in Roederer et al. (2010).

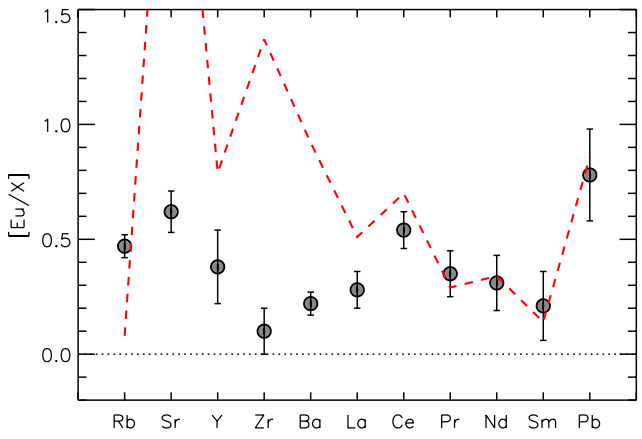

Figure 10. Abundance ratios [Eu/X] for X = Rb to Pb. The dashed red line represents the scaled-solar *r*-process distribution (Bisterzo et al. 2011). (For Sr, we apply a non-LTE correction of 0.29 dex; see Section 4.2 for details).

From Table 4, all element ratios [Eu/X] (for X = La and heavier elements) are consistent, within ∼0.2 dex, with the scaled-solar *r*-process distribution (Bisterzo et al. 2011; see Fig. 10). (Note that while we refer to *s*-process and *r*-process elements according to their origin in Solar system material, those definitions may be incorrect in M62, e.g. La and Ce in this cluster are likely produced primarily through the *r*-process.) Regarding the lighter elements, the first to

deviate from the *r*-process signature is Ba: while the solar *r*-process value is $[Eu/Ba]_r \sim 0.9$ dex, M62 exhibits a ratio of ∼0.2 dex. In the same way, all elements lighter than Ba depart from the Solar system *r*-process signature.

The neutron-capture element abundance ratios of the M62 stars are not consistent with *s*-process nucleosynthesis occurring in AGB stars of low metallicity. Low-mass AGB stars of $M \lesssim 3\,M_\odot$ are the main site of the *s*-process in the Galaxy and typically produce [hs/ls][7] ≈ 0.4, [Pb/hs] ≥ 1.0 dex and [Rb/Zr] ≤ 0 at [Fe/H] ≈ −1.2 (e.g. Busso et al. 2001; Cristallo et al. 2011; Fishlock et al., in preparation). This is a direct consequence of the operation of the $^{13}C(\alpha,n)^{16}O$ reaction which is the dominant neutron source for $M \lesssim 3\,M_\odot$ (e.g. Busso et al. 1999; Lugaro et al. 2012; Bisterzo et al. 2012). For intermediate-mass AGB stars the $^{22}Ne(\alpha,n)^{25}Mg$ reaction is the neutron source and operates during convective thermal pulses. The abundance pattern produced in those stars should be dominated by lighter *s*-process elements (Y, Rb, Sr, Zr) (van Raai et al. 2012; Karakas et al. 2012). At [Fe/H] ≈ −1.2, typical abundances in stars $M \gtrsim 3\,M_\odot$ are [hs/ls] ≈ −0.8, [Pb/hs] ≈ −0.2, and [Rb/Zr] $\gtrsim$ 0.0 dex (Fishlock et al., in preparation).

Fast-rotating massive stars (which we hereafter refer to interchangeably as 'spin stars') can produce a large amount of *s*-process products at low metallicity, where the dominant neutron source is $^{22}Ne(\alpha,n)^{25}Mg$ in the convective He-burning core and in the subsequent convective C-burning shell (Pignatari et al. 2008; Frischknecht, Hirschi & Thielemann 2012). In these stars, ^{22}Ne is primary, i.e. it is not directly produced from the initial CNO abundances as in non-rotating massive stars (see e.g. the weak *s*-process in massive stars at solar metallicity, e.g. The, El Eid & Meyer 2007; Pignatari et al. 2010). The faster the star rotates, the more primary ^{22}Ne can be made available in the He core. The most abundant elements from the *s*-process in spin stars are Sr, Y and Zr while production for heavier elements up to Ba strongly depends on the rotation speed and on nuclear uncertainties, e.g. on the α-capture rates on ^{22}Ne (Pignatari et al. 2008) and on the α-capture rates on ^{17}O (e.g. Best et al. 2013). The *s*-process in massive stars cannot produce elements beyond the Ba neutron-magic peak ($N = 82$) due to basic properties of ^{22}Ne as a neutron source (e.g. Pignatari et al. 2013).

Spin stars have been suggested as the source of the light element abundance variations in globular clusters (Decressin et al. 2007). Recall that in Fig. 6 there was no significant correlation between the abundances of Na and the neutron-capture elements. Thus, there is no obvious connection between the star-to-star Na abundance variation and the enhancement in Y, Zr and Ba abundances in this cluster.

Pignatari et al. (2008) explored the impact of changing the amount of primary ^{22}Ne available to make neutrons, from 1 per cent (in mass fraction) to 0.2 per cent, for a $25\,M_\odot$ model at [Fe/H] = −3. The result of this change was an increase in the [Zr/Ba] ratio from −0.18 to 0.67. As expected, Eu is not efficiently produced by the *s*-process regardless of the initial abundance of ^{22}Ne. M62 stars exhibit an average [Eu/Ba] = +0.2, and this value lies between the *s*-process abundance signature of spin stars and the *r*-process. This intermediate value may be a consequence of the combination of the *r*-process (which makes Eu and some Ba) and the *s*-process in spin stars (producing Ba and only a small amount of Eu).

[7] *hs* refers to the heavy *s*-process elements (Ba, La, etc.) and *ls* refers to the light *s*-process elements (Y, Zr, etc.).

M62 exhibits [Rb/Zr] and [Rb/Y] ratios of ∼−0.4 and ∼−0.1, respectively. In the models considered by Pignatari et al. (2008), reducing the initial ^{22}Ne abundance from 1 per cent (in mass fraction) to 0.2 per cent increases the [Rb/Zr] ratio from −0.86 to −0.57, and the [Rb/Y] ratio from −0.86 to −0.75. The predicted [Rb/Zr] ratio is slightly lower than the observations. Those predictions were based on a $25\,M_\odot$ spin star model. It would be of great interest to explore a larger range of initial masses in order to quantify the final core-collapse supernova yields for the elements from Rb to Zr. On the other hand, it is difficult to reconcile the average [Rb/Y] observed in M62 with spin star nucleosynthesis. Y is efficiently produced at high neutron densities from Sr. The dispersion in the [Y/Fe] ratio is consistent with the measurement uncertainties, although there is a hint that the [Y/Fe] ratios cluster around two values, ∼0.1 and ∼0.4.

The abundance enhancement at Y and Zr is a key feature of the lighter element primary process (LEPP) exhibited by some halo stars at lower metallicities, [Fe/H] $\lesssim -2$ (e.g. Travaglio et al. 2004). While the astrophysical site of the LEPP is not clearly understood, a number of scenarios have been proposed, including explosive nucleosynthesis triggered by neutrino-winds in core-collapse supernovae (e.g. Woosley & Hoffman 1992; Fröhlich et al. 2006; Farouqi et al. 2009; Arcones & Montes 2011) and the *s*-process in fast-rotating massive stars (e.g. Pignatari et al. 2008). While the aforementioned LEPP explosive scenarios cannot efficiently contribute to elements up to the Ba peak, the *s*-process in spin stars may potentially produce them.

To summarize, while the abundance ratios for the elements Y, Zr and Ba may be consistent with the *s*-process in spin stars, the high [Rb/Y] ratio is difficult to explain. Spin-star models at metallicities closer to that of M62 and for a larger range of initial masses would be needed to perform a consistent chemical evolution study, and test the spin stars scenario for this cluster.

In this context, it has been reported that NGC 6522, a bulge globular cluster, has enhanced Sr and Y abundances consistent with spin star nucleosynthesis (Chiappini et al. 2011). In that study, the abundances were derived from the Sr I 6503.99 Å and Y II 6613.73 Å lines. As noted in their paper, the Sr I line is weak. We suspect that this Y II line is blended with the Fe I 6613.82 Å line (Nave et al. 1994), and this Fe line has a lower excitation potential and log *gf* value of 1.011 eV and −5.587, respectively (Vienna Atomic Line Database; Kupka et al. 1999). It would therefore be interesting to re-examine the Sr and Y abundances in NGC 6522 using additional lines to confirm the Sr and Y enhancements in that cluster.

4.3 The lack of abundance dispersions

Our analysis reveals no evidence for an intrinsic metallicity dispersion in M62. As noted in the Introduction, the globular clusters with metallicity dispersions are preferentially the more luminous objects and tend to have extended horizontal branches. Some, and perhaps all, of these clusters may be the nuclei of accreted dwarf galaxies. Based on our results, M62 is a massive globular cluster with an extended horizontal branch that does not harbour a metallicity dispersion.

Star A124 has lower ratios of the neutron-capture elements when compared to the other program stars. Although A124 has stellar parameters and a radial velocity consistent with cluster membership, the Besançon model (Robin et al. 2003) predicts that some field contamination is likely, ∼4 per cent. The simplest explanation is that A124 is a field star. The O and Na abundances for A124 lie at the lower end of the distribution defined by the cluster stars and are similar to field stars. Proper-motion and/or parallax measurements

will test this hypothesis. Nevertheless, future studies may reveal additional stars in M62 with a range of neutron-capture element abundances. If M62 really hosts two populations of stars, of equal size, with distinct neutron-capture element abundances, then the probability of observing six out of seven program stars from a single population is 6 per cent.

5 CONCLUDING REMARKS

In this paper we present a chemical abundance analysis of seven bright giants in M62, a luminous globular cluster with an extended horizontal branch. We find no evidence for a metallicity dispersion, as seen in other luminous globular clusters with similar horizontal branch morphology. We find star-to-star abundance variations and correlations for O, Na and Al and the amplitudes of those variations are comparable to those found in the most massive globular clusters. The elements Zr, Ba and La exhibit enhancements, [X/Fe] $\sim$ +0.4, compared to field stars at the same metallicity. The lack of a significant correlation between the abundances of Na and the neutron-capture elements would suggest that the light element variations and enhancement in Y, Zr and Ba are produced in different processes and/or sites.

For the elements heavier than La, the abundances are consistent with the scaled-solar *r*-process distribution. On the other hand, Y, Zr and Ba are clearly enhanced when compared to the scaled-solar *r*-process distribution. The abundance pattern for these elements is incompatible with the s-process in AGB stars or in non-rotating massive stars. On the other hand, while the abundance distribution for these elements could be produced by fast-rotating massive stars, the high [Rb/Y] ratios that we measure do not match existing FRMS model predictions.

One star has neutron-capture element abundance ratios that are distinct from the remaining stars. While this is likely a field halo star, the identification of additional stars in the vicinity of M62 with similar abundance patterns would be of great interest. Studies of other luminous globular clusters are necessary to complete the census and characterization of the most luminous clusters in the Milky Way.

ACKNOWLEDGEMENTS

We thank Christian Johnson for helpful discussions. DY, AAB, GDC, AIK and JEN gratefully acknowledge support from the Australian Research Council (grants DP0984924, FS110200016, FT110100475 and DP120101237). JA-G acknowledges support by the Chilean Ministry for the Economy, Development, and Tourism's Programa Iniciativa Científica Milenio through grant P07-021-F, awarded to The Milky Way Millennium Nucleus; by Proyecto Fondecyt Postdoctoral 3130552; by Proyecto Fondecyt Regular 1110326; and by Proyecto Basal PFB-06/2007. MP acknowledges support from the Ambizione grant of the SNSF (Switzerland) and EuroGenesis (MASCHE). Funding for the Stellar Astrophysics Centre is provided by The Danish National Research Foundation. The research is supported by the ASTERISK project (ASTERoseismic Investigations with SONG and Kepler) funded by the European Research Council (Grant agreement no.: 267864).

REFERENCES

Alcaino G., 1978, A&AS, 32, 379
Allen C., Moreno E., Pichardo B., 2006, ApJ, 652, 1150
Allende Prieto C., Barklem P. S., Lambert D. L., Cunha K., 2004, A&A, 420, 183
Alonso-García J., Mateo M., Sen B., Banerjee M., von Braun K., 2011, AJ, 141, 146
Alonso-García J., Mateo M., Sen B., Banerjee M., Catelan M., Minniti D., von Braun K., 2012, AJ, 143, 70
Alves-Brito A., Yong D., Meléndez J., Vásquez S., Karakas A. I., 2012, A&A, 540, A3
Arcones A., Montes F., 2011, ApJ, 731, 5
Asplund M., Grevesse N., Sauval A. J., Scott P., 2009, ARA&A, 47, 481
Barbuy B. et al., 2006, A&A, 449, 349
Barbuy B., Zoccali M., Ortolani S., Minniti D., Hill V., Renzini A., Bica E., Gómez A., 2007, AJ, 134, 1613
Barbuy B., Zoccali M., Ortolani S., Hill V., Minniti D., Bica E., Renzini A., Gómez A., 2009, A&A, 507, 405
Beer H., Macklin R. L., 1989, ApJ, 339, 962
Bekki K., Freeman K. C., 2003, MNRAS, 346, L11
Bekki K., Norris J. E., 2006, ApJ, 637, L109
Bellazzini M. et al., 2008, AJ, 136, 1147
Bensby T. et al., 2013, A&A, 549, A147
Bergemann M., Hansen C. J., Bautista M., Ruchti G., 2012, A&A, 546, A90
Bernstein R., Shectman S. A., Gunnels S. M., Mochnacki S., Athey A. E., 2003, in Iye M., Moorwood A. F. M., eds, Proc. SPIE Vol. 4841, Society of Photo-Optical Instrumentation Engineers. SPIE, Bellingham, p. 1694
Best A. et al., 2013, Phys. Rev. C, 87, 045805
Biemont E., Grevesse N., Hannaford P., Lowe R. M., 1981, ApJ, 248, 867
Biemont E., Baudoux M., Kurucz R. L., Ansbacher W., Pinnington E. H., 1991, A&A, 249, 539
Biémont É. et al., 2011, MNRAS, 414, 3350
Bisterzo S., Gallino R., Straniero O., Cristallo S., Käppeler F., 2011, MNRAS, 418, 284
Bisterzo S., Gallino R., Straniero O., Cristallo S., Käppeler F., 2012, MNRAS, 422, 849
Blackwell D. E., Ibbetson P. A., Petford A. D., Shallis M. J., 1979a, MNRAS, 186, 633
Blackwell D. E., Petford A. D., Shallis M. J., 1979b, MNRAS, 186, 657
Blackwell D. E., Petford A. D., Shallis M. J., Simmons G. J., 1980, MNRAS, 191, 445
Blackwell D. E., Booth A. J., Haddock D. J., Petford A. D., Leggett S. K., 1986, MNRAS, 220, 549
Blackwell D. E., Lynas-Gray A. E., Smith G., 1995, A&A, 296, 217
Busso M., Gallino R., Wasserburg G. J., 1999, ARA&A, 37, 239
Busso M., Gallino R., Lambert D. L., Travaglio C., Smith V. V., 2001, ApJ, 557, 802
Carretta E., 2006, AJ, 131, 1766
Carretta E., Gratton R. G., 1997, A&AS, 121, 95
Carretta E., Bragaglia A., Gratton R., D'Orazi V., Lucatello S., 2009, A&A, 508, 695
Carretta E. et al., 2010a, ApJ, 714, L7
Carretta E., Bragaglia A., Gratton R. G., Recio-Blanco A., Lucatello S., D'Orazi V., Cassisi S., 2010b, A&A, 516, A55
Carretta E., Lucatello S., Gratton R. G., Bragaglia A., D'Orazi V., 2011, A&A, 533, A69
Carretta E. et al., 2013, A&A, 557, A138
Castelli F., Kurucz R. L., 2003, in Piskunov N., Weiss W. W., Gray D. F., eds, ASP Conf. Ser. IAU Symp. 210, Modelling of Stellar Atmospheres. Astron. Soc. Pac., San Francisco, p. A20
Chiappini C., Frischknecht U., Meynet G., Hirschi R., Barbuy B., Pignatari M., Decressin T., Maeder A., 2011, Nature, 472, 454
Cocozza G., Ferraro F. R., Possenti A., Beccari G., Lanzoni B., Ransom S., Rood R. T., D'Amico N., 2008, ApJ, 679, L105
Cohen J. G., Kirby E. N., 2012, ApJ, 760, 86
Cohen J. G., Kirby E. N., Simon J. D., Geha M., 2010, ApJ, 725, 288
Cohen J. G., Huang W., Kirby E. N., 2011, ApJ, 740, 60
Contreras R., Catelan M., Smith H. A., Pritzl B. J., Borissova J., Kuehn C. A., 2010, AJ, 140, 1766
Cristallo S. et al., 2011, ApJS, 197, 17

D'Antona F., Caloi V., Montalbán J., Ventura P., Gratton R., 2002, A&A, 395, 69
D'Orazi V., Gratton R. G., Pancino E., Bragaglia A., Carretta E., Lucatello S., Sneden C., 2011, A&A, 534, A29
D'Orazi V., Lugaro M., Campbell S. W., Bragaglia A., Carretta E., Gratton R. G., Lucatello S., D'Antona F., 2013, ApJ, 776, 59
Da Costa G. S., Marino A. F., 2011, Publ. Astron. Soc. Aust., 28, 28
Da Costa G. S., Held E. V., Saviane I., Gullieuszik M., 2009, ApJ, 705, 1481
De Angeli F., Piotto G., Cassisi S., Busso G., Recio-Blanco A., Salaris M., Aparicio A., Rosenberg A., 2005, AJ, 130, 116
de Mink S. E., Pols O. R., Langer N., Izzard R. G., 2009, A&A, 507, L1
Decressin T., Meynet G., Charbonnel C., Prantzos N., Ekström S., 2007, A&A, 464, 1029
Den Hartog E. A., Lawler J. E., Sneden C., Cowan J. J., 2003, ApJS, 148, 543
Dinescu D. I., Girard T. M., van Altena W. F., 1999, AJ, 117, 1792
Dinescu D. I., Girard T. M., van Altena W. F., López C. E., 2003, AJ, 125, 1373
Farouqi K., Kratz K.-L., Mashonkina L. I., Pfeiffer B., Cowan J. J., Thielemann F.-K., Truran J. W., 2009, ApJ, 694, L49
Fenner Y., Campbell S., Karakas A. I., Lattanzio J. C., Gibson B. K., 2004, MNRAS, 353, 789
Ferraro F. R. et al., 2009, Nature, 462, 483
Freeman K. C., 1993, in Smith G. H., Brodie J. P., eds, ASP Conf. Ser. Vol. 48, The Globular Cluster-Galaxy Connection, Astron. Soc. Pac., San Francisco, p. 608
Freeman K., Bland-Hawthorn J., 2002, ARA&A, 40, 487
Frischknecht U., Hirschi R., Thielemann F.-K., 2012, A&A, 538, L2
Fröhlich C., Martínez-Pinedo G., Liebendörfer M., Thielemann F.-K., Bravo E., Hix W. R., Langanke K., Zinner N. T., 2006, Phys. Rev. Lett., 96, 142502
Fuhr J. R., Wiese W. L., 2009, in CRC Handbook of Chemistry and Physics, 90th edn. CRC Press, Boca Raton, p. 10
Fulbright J. P., 2000, AJ, 120, 1841
Gallino R., Arlandini C., Busso M., Lugaro M., Travaglio C., Straniero O., Chieffi A., Limongi M., 1998, ApJ, 497, 388
García-Hernández D. A., García-Lario P., Plez B., D'Antona F., Manchado A., Trigo-Rodríguez J. M., 2006, Science, 314, 1751
García-Hernández D. A. et al., 2009, ApJ, 705, L31
Goriely S., Mowlavi N., 2000, A&A, 362, 599
Gratton R. G., Carretta E., Claudi R., Lucatello S., Barbieri M., 2003, A&A, 404, 187
Gratton R., Sneden C., Carretta E., 2004, ARA&A, 42, 385
Gratton R. G., Carretta E., Bragaglia A., 2012, A&AR, 20, 50
Gustafsson B., Bell R. A., Eriksson K., Nordlund A., 1975, A&A, 42, 407
Harris W. E., 1996, AJ, 112, 1487
Ivans I. I., Sneden C., Kraft R. P., Suntzeff N. B., Smith V. V., Langer G. E., Fulbright J. P., 1999, AJ, 118, 1273
Ivans I. I., Kraft R. P., Sneden C., Smith G. H., Rich R. M., Shetrone M., 2001, AJ, 122, 1438
Ivans I. I., Sneden C., Gallino R., Cowan J. J., Preston G. W., 2005, ApJ, 627, L145
Johnson C. I., Pilachowski C. A., 2010, ApJ, 722, 1373
Johnson C. I., Rich R. M., Kobayashi C., Fulbright J. P., 2012, ApJ, 749, 175
Kappeler F., Beer H., Wisshak K., 1989, Rep. Progress Phys., 52, 945
Karakas A. I., García-Hernández D. A., Lugaro M., 2012, ApJ, 751, 8
Kraft R. P., 1994, PASP, 106, 553
Kraft R. P., Ivans I. I., 2003, PASP, 115, 143
Kupka F., Piskunov N., Ryabchikova T. A., Stempels H. C., Weiss W. W., 1999, A&AS, 138, 119
Kurucz R., Bell B., 1995, Atomic Line Data (R.L. Kurucz and B. Bell) Kurucz CD-ROM No. 23. Smithsonian Astrophysical Observatory, Cambridge, p. 23
Lambert D. L., Luck R. E., 1976, The Observatory, 96, 100
Lanzoni B. et al., 2010, ApJ, 717, 653
Lardo C., Pancino E., Mucciarelli A., Milone A. P., 2012, A&A, 548, A107
Lardo C. et al., 2013, MNRAS, 433, 1941
Lawler J. E., Bonvallet G., Sneden C., 2001a, ApJ, 556, 452
Lawler J. E., Wickliffe M. E., den Hartog E. A., Sneden C., 2001b, ApJ, 563, 1075
Lawler J. E., Den Hartog E. A., Sneden C., Cowan J. J., 2006, ApJS, 162, 227
Lawler J. E., Sneden C., Cowan J. J., Ivans I. I., Den Hartog E. A., 2009, ApJS, 182, 51
Lee Y.-W., Gim H. B., Casetti-Dinescu D. I., 2007, ApJ, 661, L49
Li R., Chatelain R., Holt R. A., Rehse S. J., Rosner S. D., Scholl T. J., 2007, Phys. Scr, 76, 577
Lugaro M., Karakas A. I., Stancliffe R. J., Rijs C., 2012, ApJ, 747, 2
McWilliam A., Rich R. M., 1994, ApJS, 91, 749
Marcolini A., Gibson B. K., Karakas A. I., Sánchez-Blázquez P., 2009, MNRAS, 395, 719
Marino A. F., Villanova S., Piotto G., Milone A. P., Momany Y., Bedin L. R., Medling A. M., 2008, A&A, 490, 625
Marín-Franch A. et al., 2009, ApJ, 694, 1498
Marino A. F., Milone A. P., Piotto G., Villanova S., Bedin L. R., Bellini A., Renzini A., 2009, A&A, 505, 1099
Marino A. F. et al., 2011, A&A, 532, A8
Mucciarelli A., Bellazzini M., Ibata R., Merle T., Chapman S. C., Dalessandro E., Sollima A., 2012, MNRAS, 426, 2889
Nave G., Johansson S., Learner R. C. M., Thorne A. P., Brault J. W., 1994, ApJS, 94, 221
Noguchi K. et al., 2002, PASJ, 54, 855
Norris J. E., Da Costa G. S., 1995, ApJ, 447, 680
Norris J. E., Yong D., Gilmore G., Wyse R. F. G., 2010, ApJ, 711, 350
Origlia L. et al., 2011, ApJ, 726, L20
Origlia L., Massari D., Rich R. M., Mucciarelli A., Ferraro F. R., Dalessandro E., Lanzoni B., 2013, ApJ, 779, L5
Otsuki K., Honda S., Aoki W., Kajino T., Mathews G. J., 2006, ApJ, 641, L117
Pignatari M., Gallino R., Meynet G., Hirschi R., Herwig F., Wiescher M., 2008, ApJ, 687, L95
Pignatari M., Gallino R., Heil M., Wiescher M., Käppeler F., Herwig F., Bisterzo S., 2010, ApJ, 710, 1557
Pignatari M. et al., 2013, ApJ, 762, 31
Piotto G. et al., 2002, A&A, 391, 945
Prochaska J. X., Naumov S. O., Carney B. W., McWilliam A., Wolfe A. M., 2000, AJ, 120, 2513
Ramírez S. V., Cohen J. G., 2002, AJ, 123, 3277
Robin A. C., Reylé C., Derrière S., Picaud S., 2003, A&A, 409, 523
Roederer I. U., Lawler J. E., 2012, ApJ, 750, 76
Roederer I. U., Cowan J. J., Karakas A. I., Kratz K.-L., Lugaro M., Simmerer J., Farouqi K., Sneden C., 2010, ApJ, 724, 975
Roederer I. U., Marino A. F., Sneden C., 2011, ApJ, 742, 37
Roederer I. U. et al., 2012, ApJS, 203, 27
Rutledge G. A., Hesser J. E., Stetson P. B., Mateo M., Simard L., Bolte M., Friel E. D., Copin Y., 1997, PASP, 109, 883
Saviane I., Da Costa G. S., Held E. V., Sommariva V., Gullieuszik M., Barbuy B., Ortolani S., 2012, A&A, 540, A27
Simmerer J., Ivans I. I., Filler D., Francois P., Charbonnel C., Monier R., James G., 2013, ApJ, 764, L7
Skrutskie M. F. et al., 2006, AJ, 131, 1163
Smith V. V., Suntzeff N. B., Cunha K., Gallino R., Busso M., Lambert D. L., Straniero O., 2000, AJ, 119, 1239
Sneden C., 1973, ApJ, 184, 839
Sneden C., Johnson J., Kraft R. P., Smith G. H., Cowan J. J., Bolte M. S., 2000, ApJ, 536, L85
Sobeck J. S. et al., 2011, AJ, 141, 175
Stetson P. B., Pancino E., 2008, PASP, 120, 1332
The L.-S., El Eid M. F., Meyer B. S., 2007, ApJ, 655, 1058
Travaglio C., Gallino R., Arnone E., Cowan J., Jordan F., Sneden C., 2004, ApJ, 601, 864
Valenti E., Ferraro F. R., Origlia L., 2007, AJ, 133, 1287
Van Eck S., Goriely S., Jorissen A., Plez B., 2001, Nature, 412, 793
van Raai M. A., Lugaro M., Karakas A. I., García-Hernández D. A., Yong D., 2012, A&A, 540, A44

VandenBerg D. A., Brogaard K., Leaman R., Casagrande L., 2013, ApJ, 775, 134
Ventura P., D'Antona F., 2005, ApJ, 635, L149
Villanova S., Geisler D., Piotto G., 2010, ApJ, 722, L18
Woosley S. E., Hoffman R. D., 1992, ApJ, 395, 202
Worley C. C., Hill V., Sobeck J., Carretta E., 2013, A&A, 553, A47
Yong D., Grundahl F., 2008, ApJ, 672, L29
Yong D., Grundahl F., Nissen P. E., Jensen H. R., Lambert D. L., 2005, A&A, 438, 875
Yong D., Aoki W., Lambert D. L., Paulson D. B., 2006, ApJ, 639, 918
Yong D., Lambert D. L., Paulson D. B., Carney B. W., 2008a, ApJ, 673, 854
Yong D., Karakas A. I., Lambert D. L., Chieffi A., Limongi M., 2008b, ApJ, 689, 1031
Yong D. et al., 2013, MNRAS, 434, 3542
Zinn R., West M. J., 1984, ApJS, 55, 45

SUPPORTING INFORMATION

Additional Supporting Information may be found in the online version of this article

Table 2. Line list and EWs.
Table 3. Chemical abundances for the program stars.
(http://mnras.oxfordjournals.org/lookup/suppl/doi:10.1093/mnras/stu118/-/DC1).

Please note: Oxford University Press is not responsible for the content or functionality of any supporting materials supplied by the authors. Any queries (other than missing material) should be directed to the corresponding author for the article.

This paper has been typeset from a TEX/LATEX file prepared by the author.